The sperm hook in house mice: a functional adaptation for migration and self-organised behaviour

Short title: Mouse sperm behaviour in the female reproductive tract

Heungjin Ryu[1,2]*†, Kibum Nam[1]†, Byeong Eun Lee[3]†, Yundon Jeong[1]†, Seunghun Lee[1], Jeongmo Kim[1], Young-Min Hyun[4], Jae-Ick Kim[3]*, Jung-Hoon Park[1]*

1. Department of Biomedical Engineering, Ulsan National Institute of Science and Technology; Ulju-gun, Ulsan, 44919, Republic of Korea

2. Department of Social Informatics, Kyoto University; Sakyo-ku, Kyoto 606-8501, JAPAN

3. Department of Biological Sciences, Ulsan National Institute of Science and Technology; Ulju-gun, Ulsan, 44919, Republic of Korea

4. Department of Anatomy, Yonsei University College of Medicine, Seoul, 03722, Republic of Korea

*Corresponding authors. Heungjin Ryu, Jae-Ick Kim, Jung-Hoon Park

Corresponding authors' email**:** ryu.heungjin.26v@kyoto-u.jp; jikim220@unist.ac.kr; jh.park@unist.ac.kr

Abstract

Mouse sperm has a falciform apical hook at the head of the sperm. In this study, we investigated the function of the sperm hook while migrating through the female reproductive tract in *Mus musculus* (C57BL/6), using custom-built two-photon microscopy. Our observations indicate that sperm hook plays a probe-like role to facilitate sperm interaction with the epithelium during migration and an anchor-like role to secure onto the epithelia of the uterine and oviduct. We found no direct evidence of sperm trains being beneficial in their migration. While the sperm hook may be a key for sperm cooperative behaviour in other rodent species, our results suggest that in house mice, the sperm hook plays a role in sperm migration through female reproductive tract, but not for cooperative behaviour, except for synchronised sperm beating.

Keywords: kinetics, mouse, sperm hook, sperm train, sperm migration, two-photon microscope, female reproductive tract

Introduction

A unique morphological feature of murine sperm is the apical hook resulting in an asymmetrical falciform head shape [1]. The functional benefit of this asymmetrical sperm hook structure is still debated in the field of mouse reproductive ecology. Currently, two main hypotheses attempt to explain the function of the sperm hook. One suggests that the sperm hook plays a crucial role in

sperm competition by aiding sperm train formation – the sperm cooperation hypothesis [2,3]. The other proposes that the sperm hook plays a significant role in sperm migration in the female reproductive tract – the migration hypothesis [4,5]. Since the pioneering discovery of organized sperm accumulation known as sperm trains [2], some researchers have demonstrated in vitro that the sperm train facilitates faster or straighter sperm swimming [2,3]. However, other studies could not find supporting evidence of sperm cooperation by sperm accumulation or species-specific morphological changes of sperm hooks concerning the degree of sperm competition [5,6]. These researchers rather suggest that the sperm hook plays a crucial role in sperm migration by interacting with epithelia in the female reproductive tract.

Testing these hypotheses require direct observation of live sperm within the intact female reproductive tract. In this study, we developed an ex-vivo observation system based on a custom-built two-photon microscope and investigated sperm migration in live female reproductive tracts (Fig. S1). Two-photon microscopy is currently the method of choice for live imaging of deep tissues [7–9]. However, it has seldom been used for studying animal reproductive ecology. As the mouse oviduct is made up of thin muscle layers, it is more transparent than the uterus. Most previous studies, therefore, targeted observation of the oviduct using brightfield, fluorescence or confocal microscopy [10–12]. However, as the mouse uterus has thicker muscle layers making it opaque, direct observation of the sperm behaviour in the uterus, which is crucial to understand the role of the apical sperm hook in sperm migration, has been lacking. Here, we demonstrate high-resolution deep-tissue imaging that allows us to observe and track sperm movement inside the female reproductive tract including the uterus to realize real-time tracking of sperm and their migration. We report newly discovered sperm behaviour and aggregation patterns that suggest various roles of mouse sperm hook in migration inside the female reproductive tract.

Results

Variations in sperm swimming near the uterus wall

To study sperm behaviour in the female reproductive tract, we mated wild-type females with transgenic male mice (Tables S1 and S2) that express DsRed at the sperm mid-piece (mitochondria) and eGFP in the sperm acrosome [13]. The female mice were euthanized between 0.5 and 3 hours post-mating, and their reproductive tract with copulatory plug was excised and transferred to a sterilized Petri dish. We then conducted *ex-vivo* imaging of the live reproductive tract using our two-photon microscope. All observations were typically completed within 3 hours and did not exceed 6 hours post-euthanasia. Despite this observation period being longer than recommended for conventional rat transplantation surgery [14], we noted live uterine movements throughout the entire observation period. When samples were transferred to incubators preheated to 37°C with 5% CO_2 following observation, uterine movement persisted even 24 hours post-excision. We used Fiji [15] and R [16] for image processing and statistical analysis.

We first observed sperm movement in the uterus, where the majority of ejaculated sperm were located and where initial sperm selection occurs. In the uterus, we observed vigorous fluid flow caused by uterine contraction and relaxation. Consequently, most sperm in the uterus were carried by this flow, adhering to the inherent flow dynamics within the uterus (Movie S1A). However, during periods when the flow temporarily ceased, we were able to observe active

sperm swimming in the uterus. We noted that sperm located near the uterine wall exhibited greater activity (Movie S1B). To quantitatively compare sperm speed and sperm swimming trajectory characteristics relative to their distance from the uterine wall, we employed the TrackMate plugin in ImageJ [17,18] for sperm tracking. After successful tracking using the customized tracking option in TrackMate, we computed various sperm kinetics parameters. These parameters included the curvilinear velocity (VCL), straight-line velocity (VSL), and linearity of forward progression (LIN), which are commonly used in computer-assisted sperm analysis, CASA [19]. Briefly, VCL was calculated as total distance travelled divided by total travel time, VSL as the distance between initial and final positions of the sperm trajectory divided by total travel time, and LIN as the ratio of VSL to VCL, which can range from 0 to 100%, with 100% representing a perfectly straight line. We also introduced a new kinetics parameter called straight line-to-sideward movement ratio (SWR), defined as track displacement of a sperm trajectory divided by maximum sideward movement distance (refer to Fig. S2A and S2B for our definition of uterus wall and a schematic description of the sperm kinetics parameters, as well as Methods for more detail).

Our sperm tracking analysis revealed that sperm located close to the uterine wall moved faster, exhibiting higher VCL and VSL (Fig. 1A and Table S3). However, LIN and SWR did not significantly vary depending on sperm distance from the uterus wall (Fig. 1B). In contrast to the non-significant changes in LIN and SWR relative to distance from the uterine wall, when sperm swam parallel to the wall, they not only moved faster (higher VCL and VSL; Fig. 1A), but also followed a straighter path (higher LIN and SWR; Fig. 1B). These results suggest that migration along the uterine wall may be an efficient strategy to reach the entrance of the utero-tubal junction (UTJ), that is also called colliculus tubarius (CT).

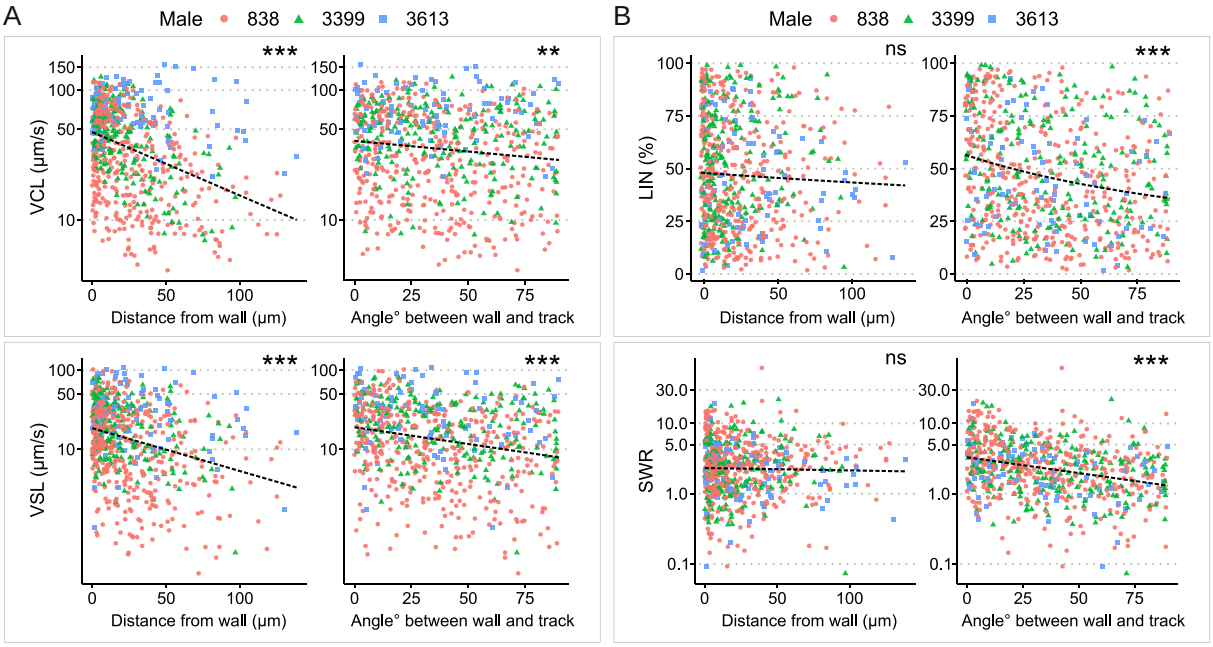

Figure 1. Analysis of sperm kinetics parameters relative to the distance and angle between the sperm trajectory and uterine wall. (**A**) Both VCL (top) and VSL (bottom) showed a decrease with

an increase in the distance between the sperm trajectory and the uterine wall. Similarly, VCL and VSL decreased as the angle between the sperm trajectory and uterine wall increased. (**B**) The distance between the sperm trajectory and uterine wall did not significantly affect LIN (top left) and SWR (bottom left). However, both LIN and SWR decreased when the angle between the sperm trajectory and uterine wall increased. Data from different males are represented in different colours and shapes. The dotted lines indicate regression lines from simple regressions to aid visual interpretation. Check model estimates for more details and precise interpretation of the models (Table S3). The y-axis of each figure is displayed in log-scale except for LIN.

The role of apical sperm head in sperm migration

Based on our observation of sperm motility in the female reproductive tract, we propose that the sperm hook may play crucial roles in determining the direction of migration in mice. When a sperm encounters the uterine wall (epithelium) during migration, the sperm hook can act as a pivot that influences the direction of sperm travel (Fig. 2A and 2B). Movie S2A illustrates two distinct types of sperm movement when transitioning from the uterus volume to the uterine wall: pro-wall-hook and anti-wall-hook directional movement (Fig. 2C). Upon reaching the uterine wall, instead of randomly deflecting in various directions, sperm preferentially altered their heading direction such that their apical hook would face the uterine wall (pro-wall-hook direction). To test whether their hook influences the direction of migration, we tracked sperm that travelled from the uterus volume to the wall in sequentially acquired images. We found that 52 out of 63 sperm (82.54%) changed their migration direction towards the pro-wall-hook direction after reaching the uterine wall (Fig. 2D). The remaining 11 sperm followed the anti-wall-hook direction. A binomial test confirmed that this tendency was statistically significant (one-tailed, $p < .001$, 95% CI: 0.73, 1.00). This result suggests that the apical sperm hook may influence sperm travel direction upon encountering uterine epithelium, as suggested in previous studies [5,10]. These findings imply that when sperm reach the uterine epithelium, they can migrate along the uterine wall. Therefore, the sperm hook may aid sperm migration direction along the uterine wall by assisting in sperm orientation.

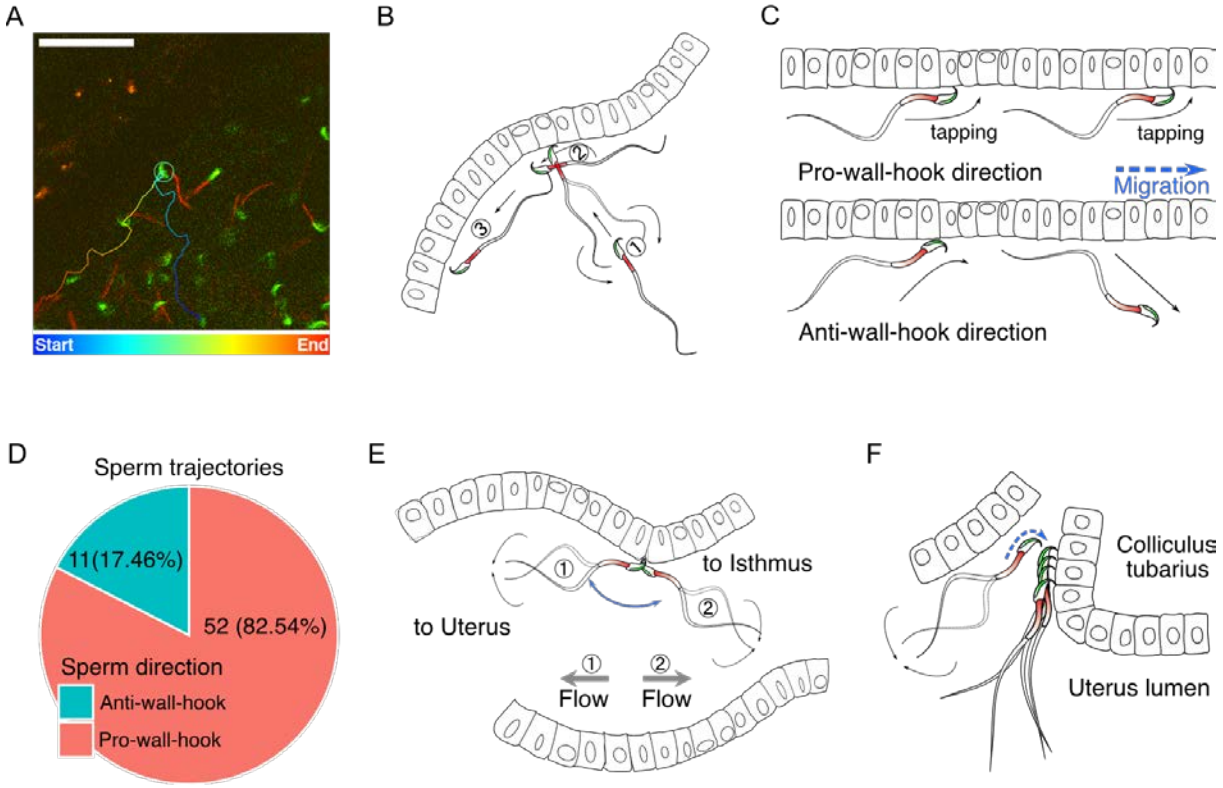

Figure 2. The sperm hook plays an important role in sperm migration through the female reproductive tract by facilitating interactions between sperm and epithelia. (**A**) Sperm alter their travel direction based on their head orientation upon reaching the uterine wall (sperm hook functions as a pivot, Movie S2A). The trajectory of a sperm cell is depicted in colours representing different time points. Scale bar: 50 µm. (**B**) The illustration shows how sperm travel direction changes. Numbers in the illustration indicate the sequences of sperm movement. (**C**) The direction of sperm travel may be influenced by the orientation of sperm hook to the wall (pro-wall or anti-wall) while they migrate along the uterine epithelium. (**D**) When sperm reach the uterine epithelium, their trajectories predominantly follow the pro-wall-hook direction, where the sperm hook is directed towards the uterine epithelium. (**E**) The sperm hook may assist a spermatozoon in anchoring to the epithelia (hook as an anchor). This anchoring may facilitate sperm attachment to the uterine and UTJ epithelium and help them resist changes in internal flow direction due to peristaltic movement. (**F**) The sperm hook and thin sperm head may aid sperm in squeezing through the sperm-crowded UTJ entrance (CT) and attaching to the epithelium by acting as an anchor (Movie S3 and Fig. S3). Note that the principal and terminal pieces of sperm in all illustrated diagrams do not represent the entire sperm shape and beating motion of the sperm tail due to a lack of fluorescence.

Furthermore, when sperm migrated along the uterine wall, they exhibit a tapping-like behaviour with their hook on the epithelium when oriented in a pro-wall-hook direction (Movie S2B). Although such tapping may be driven by tail beating, we were unable to directly observe the full dynamics in our current experiments due to a lack fluorescence in the principle and terminal pieces in our model mouse sperm. The curved hook that bends towards the tail direction, not headway direction, may also enable sperm to travel along the uterine wall while their hooks face the wall as its bent direction will not hinder headway movement. In contrast, when the sperm

hook faces the luminal space, sperm could not migrate along the wall (Fig. 2D). Instead, their migration trajectories followed the anti-wall-hook direction, resulting in movement away from the wall (Fig. 2D and Movie S2A). In addition to the advantage in straighter trajectories, fluid flows are slower at the wall than at the centre of the lumen [20], which may be beneficial for sperm migration along the uterine wall to successfully reach the entrance of the UTJ (or CT), where one of the most important sperm selection processes takes place [12,21].

When sperm reach the UTJ in the uterus, the sperm hook may aid a spermatozoon in attaching to the uterus and UTJ epithelium. The sperm hook could function as an anchor, helping sperm to secure themselves at crypts or on surfaces where small furrow-like structures exist that can jam or hold the sperm hook (Fig. 2E, Movie S3, A and B). Given that the surface of uterine wall (epithelium) possesses small furrow-like structures [22,23], such anchoring with the hook can play a significant role in successful sperm migration if the sperm hook anchor to these structures or if it helps sperm adhesion on the surface [24]. This anchoring may in turn help prevent sperm from being swept away by mucosal flow or other sperm. The complex surface structure at the entrance to the UTJ (CT) due to the presence of mucosal folds [23], along with a pointed apical sperm hook and thin head shape can also assist sperm in attaching to the CT and squeezing past other sperm by hooking (Fig. 2F and Movie S3A). Once sperm successfully cling onto CT epithelia, anchoring to the epithelia prevents them from being pushed out by competing sperm or swept away by fluid flow (Movie S3B).

Structure of UTJ and sperm passage

Upon clearing the tissue, we confirmed that the entrance to the intramural UTJ in the uterus consists of nearly closed narrow gaps between mucosal folds (Fig. 3A). These narrow gaps extended to about 100 µm deeper from the entrance (Movie S4, A and B), and their diameters are so narrow such that only a few sperm can pass through them at a time (Movie S4C). We were not able to find evidence of passive sperm carriage, such as upsuck-like movement [25], caused by peristaltic movement from the uterus into the UTJ in real-time live images (Movie S5A). Therefore, we hypothesize that fluid flow induced by uterine and oviduct contraction is not a major driving force for sperm entering the UTJ through the CT. Then how can sperm enter the UTJ through the CT if the UTJ entrance is nearly closed?

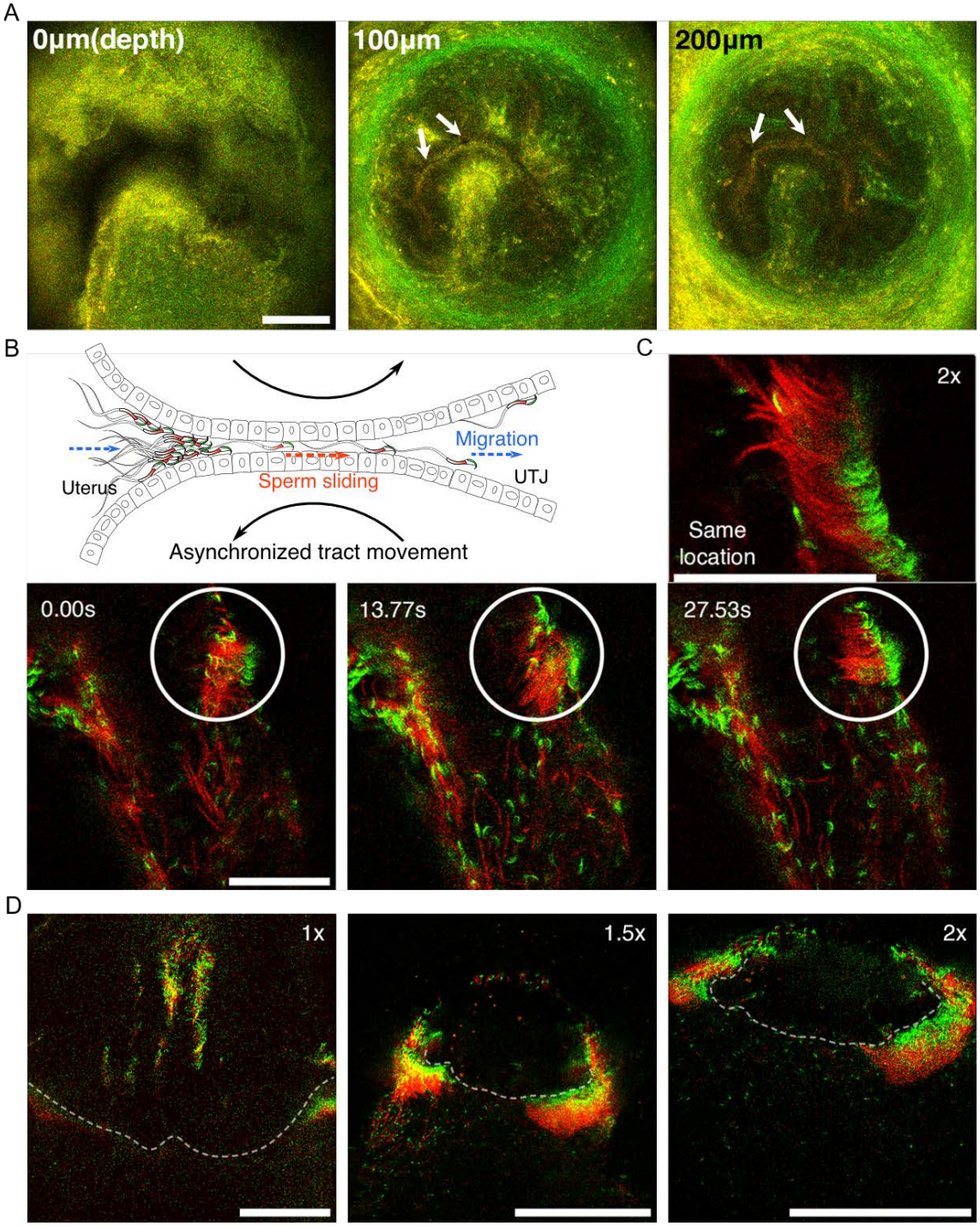

Figure 3. The apical sperm hook may facilitate sperm entry into the UTJ through the CT by aiding in sperm attachment and sliding. (**A**) The structure of the CT (entrance to the UTJ) of the intramural UTJ of an unmated female is shown. There are only a few small gaps indicated by arrows between mucosal folds, which may limit sperm migration into the UTJ from the uterus (Movie S4). Scale bar: 100 μm. (**B**) Asynchronised movement of mucosal folds at the CT due to uterine and UTJ contractions may enable sperm to penetrate or slide into the intramural UTJ from the uterus (Movie

S5). Two dashed arrows (in blue) indicate the direction of sperm migration from the uterus to the UTJ, and the dashed arrow in the centre (in orange) indicates the direction of sperm sliding in the intramural UTJ. The two curved black arrows indicate asynchronised (opposite) movement of confronting mucosal folds in the intramural UTJ. (**C**) The apical shape of the sperm head, due to the sperm hook, results in head asymmetry. This asymmetrical falciform head shape may also facilitate sperm re-arrangement and clustering at crypts in the uterus (Movie S6). The circle highlights sperm undergoing unidirectional re-arrangement over time. The elapsed time after the first frame is shown in the upper left of the images. The right upper zoom-in inset shows an instant of synchronised motion and unidirectional re-arrangement. Scale bar: 50 µm. (**D**) Unidirectional sperm clustering in the uterus at the entrance of the intramural UTJ (indicated by a dashed line) is marked with arrows. Such large sperm clustering sometimes results in synchronised sperm beating at the entrance of the UTJ (Movie S7). Scale bar: 200 µm. Note that due to a lack of fluorescence, the principal and terminal pieces of sperm in all illustrated diagrams do not represent the actual sperm shape and beating motion of the entire sperm tail.

We observed that when muscle contraction and relaxation occur at the uterus and oviduct, the surfaces of two confronting mucosal folds in intramural UTJ sometimes slide against each other in opposite directions (Fig. 3B and Movie S5B). For example, when the uterus bends to the left due to muscle contraction on its left side and relaxation of its right side, the intramural UTJ is pulled to the left by uterus contraction. This pulling may then cause elongation of mucosal folds on the left side of intramural UTJ but negligible elongation on its right-side mucosal folds (Fig. S3). Such opposite directional movement may create a small opening between inter-mucosal gaps at the entrance of the UTJ, providing an opportunity for nearby attached sperm to enter the UTJ (Movie S5B). Along with the anchoring function of the hook, the falciform apical hook may facilitate head-directional sliding as they migrate through the narrow mucosal lumen in the intramural UTJ (Movie S5C). The asymmetric shape of the mouse sperm head is advantageous as their round surface may aid migration in the forward direction (head direction), while their hooks may prevent or hinder backward movement (tail direction) by acting as anchors.

Unidirectional sperm clustering

We observed spontaneous unidirectional sperm clustering as a result of spontaneous sperm re-arrangement during sperm beating along the uterine wall (Fig. 3C and Movie S6, A and B). Such unidirectional sperm clustering and their coordinated beating can sometimes result in synchronised sperm beating. When a large number of sperm attached to the entrance to the intramural UTJ (CT) in the uterus, this sperm clustering could cause synchronised sperm beating on a large scale at the CT (Fig. 3D and Movie S7). Based on these observations, we propose that the asymmetry of the mouse sperm head due to its apical hook plays a crucial role in synchronised sperm beating by facilitating unidirectional sperm re-arrangement on the uterine wall. The synchronised sperm beating was observed to generate fluid flows strong enough to prevent other sperm from attaching to the CT or directly push out other sperm, thereby preventing other sperm from entering the UTJ (Movie S6 and S7). Therefore, asymmetrical head shapes in house mice may have evolved not only to facilitate sperm migration but also to facilitate unidirectional clustering and synchronised beating. In this scenario, sperm cooperation in house mice may not always be mediated by sperm train formation as suggested in other rodent species [2,3], but may be mediated by synchronised beating that prevents migration of rival

sperm in the uterus. In line with this argument, we found that sperm trains in the uterus did not necessary swim faster than unlinked single spermatozoa (Fig. 4A, Movie S8). Although we did not conduct a statistical test due to the small number of sperm trains observed in our experiments, the rarely observed sperm trains did not move faster than unlinked single spermatozoa, as shown in Fig. 4A and 4B. Their VCL, VSL, and LIN were not faster nor higher than those of unlinked single spermatozoa (Fig. 4B). However, it is still possible that their SWR is higher than that of unlinked sperm cells. Due to the rare number of observed events, further experiments will be needed to clarify whether the sperm train formation is advantageous in-vivo in the house mouse.

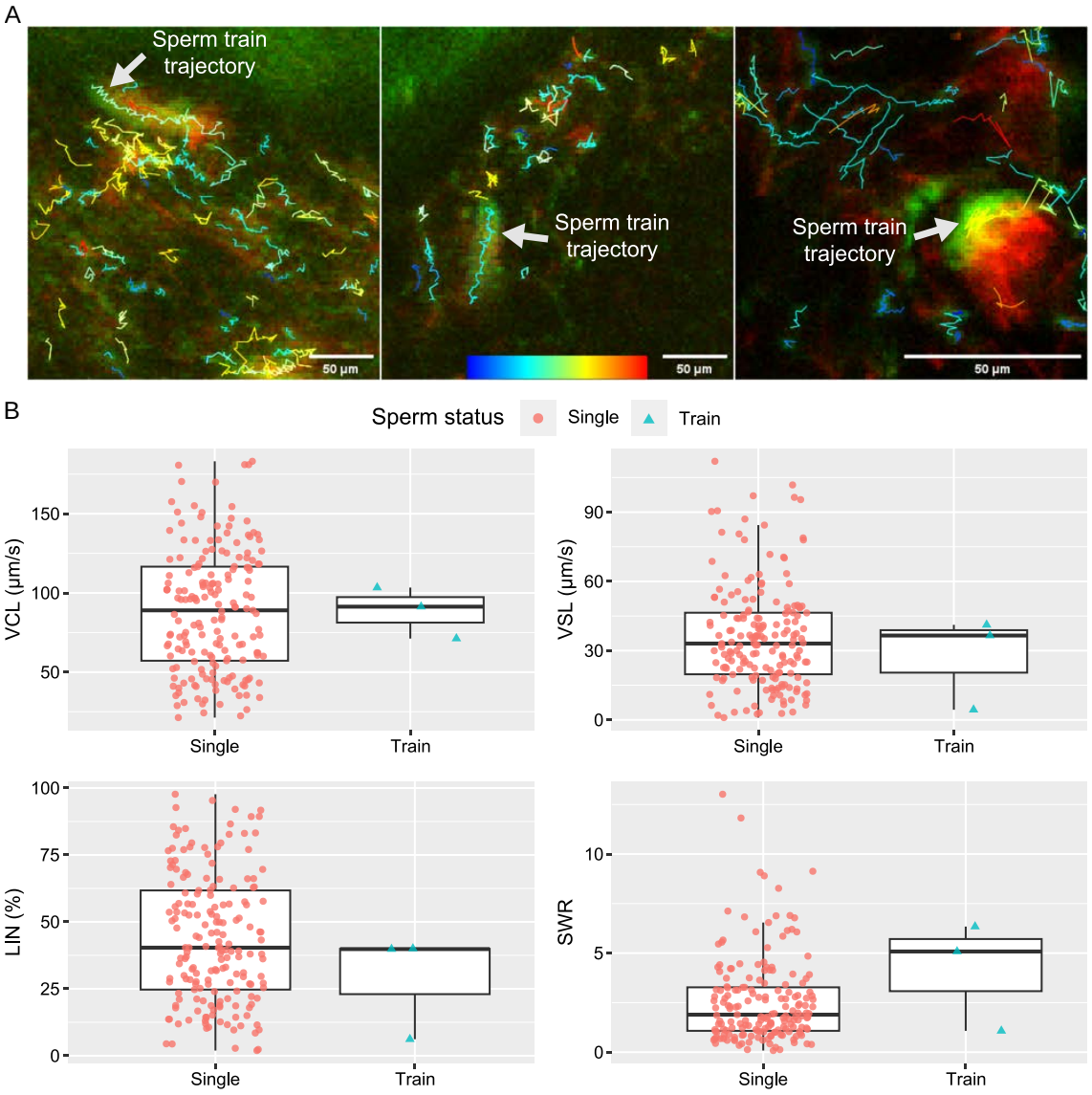

Figure 4. Comparative trajectories and kinetics of accumulated spermatozoa (sperm trains) and unlinked single spermatozoa (**A**) The projected images, comprising 60 frames, depict the trajectories of sperm trains and unlinked single spermatozoa. The colour bar located at the bottom centre represents the VCL of each sperm trajectory, with blue indicating slower speeds and red indicating

faster speeds. (**B**) The boxplots, which include individual data points, represent the kinetic parameters of the sperm trains and unlinked single spermatozoa. The parameters, including curvilinear velocity (VCL), straight-line velocity (VSL), linearity of forward progression (LIN), and straight line-to-sideward movement ratio (SWR), were computed using images of 100x100 pixels that contained a sperm train. In the few observed cases, the sperm trains did not exhibit a faster VCL or VSL, nor a higher LIN. However, it is still possible that the SWR is higher in the sperm train. The lines within the boxes represent the medians, and the whiskers represent 1.5 times the interquartile ranges, and the symbols show the individual data points.

Resisting internal flow using the apical head as an anchor

After entering the UTJ, sperm migrate through the narrow UTJ lumen. Sometimes narrow gaps between mucosal folds in the UTJ prevent sperm migration. The pointed hook and thin head shape of the sperm may help them pass through these gaps (Fig. 5A and Movie S9A). This sperm behaviour suggests another function of their hook: facilitating sperm passage through the narrow UTJ lumen after entering UTJ. The luminal width and direction of fluid flow in the UTJ change over time depending on oviduct movement (Movie S9B). When the UTJ lumen contracts, both swimming and beating of the sperm are physically suppressed (Fig. 5B). However, when the UTJ lumen dilates, the sperm can beat and start swimming again (Movie S9B). Fluid flow may still be vigorous right after expansion of the UTJ lumen. This vigorous flow can damage unattached sperm, particularly when they get entangled with accumulated sperm that are moving back and forth due to flow (Movie S9C). Therefore, it would be advantageous for sperm if they could response to fluid flow. We observed that attached sperm's beating rates may change over time according to UTJ lumen widths and flow speed (Movie S10). Although such changes in beating rate may simply reflect luminal flow speed or luminal width related to physical comfort for beating, it can also assist in attaching sperm to epithelium by providing required propulsive force. As demonstrated in a previous study, oviductal fluid gradually flows upward while continuously repeating back-and-forth directional changes [26]. Such directional fluid flow will aid in migrating from UTJ to ampulla. However, given our observation of resistant (anchoring) behaviour of sperm to flow in UTJ and isthmus, passive transfer may not be beneficial for healthy sperm. In addition, passive transfer along fast flow can cause physical damage to the sperm due to fast collision along narrow and complicated lumen structures. As bursa hole is open, passively transferred sperm can also leak out through bursa hole.

Contrary to previous findings in other rodent species such as deer and wood mice [2,3], we were unable to identify sperm trains that evidently assist sperm in swimming faster or straighter in the uterus and oviduct. As observed in previous studies on other mouse species, we found sperm accumulations (or sperm trains) of various sizes in the uterus and oviduct, including UTJ and isthmus (Fig. 5, C and D). Although we could not perform a statistical analysis, the accumulated (linked) sperm did not appear to move faster compared to nearby unlinked single sperm in the uterus (Movie S8). This observation suggests that sperm accumulation may not aid faster migration in the female reproductive tract in house mice. Instead, sperm accumulation may obstruct the migration of other sperm in the oviduct, including the UTJ and isthmus, as accumulated sperm occupy the oviductal lumen, blocking the passage of other sperm as seen in Movie S9C. Such obstruction of other sperm's migration by sperm accumulation could also play

a role in sperm competition by preventing sequential sperm migration from a second male, although more data and experiments are needed to test this possibility.

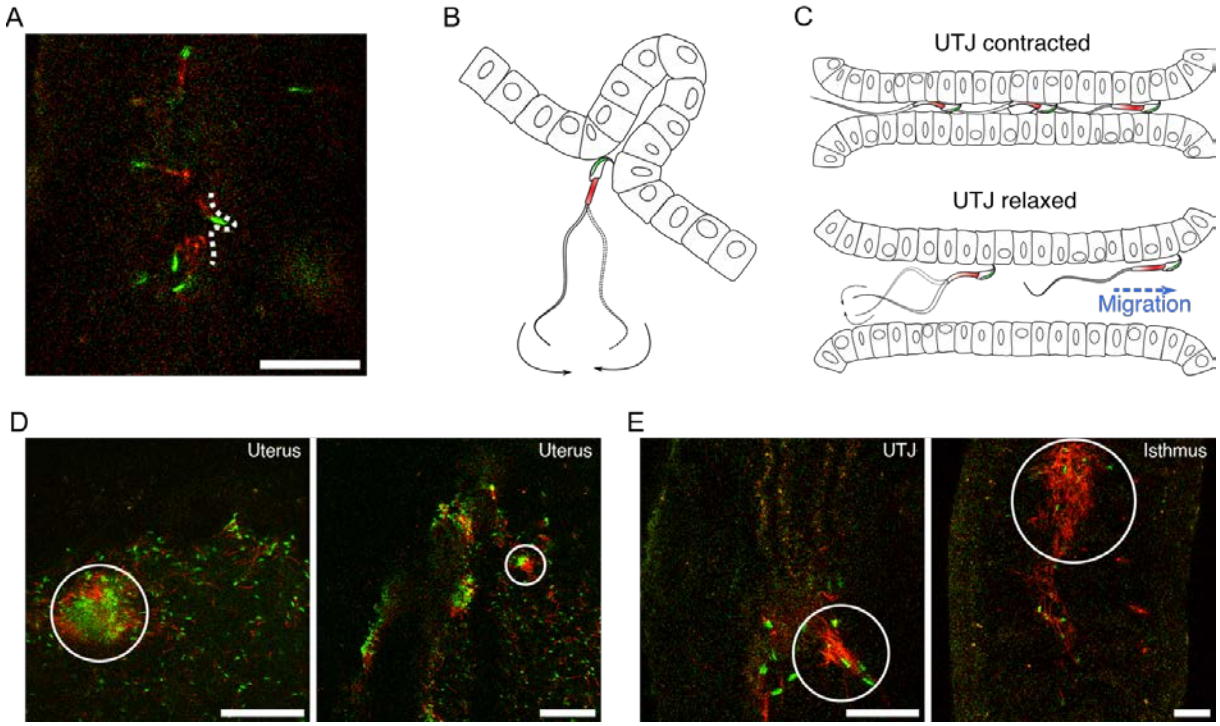

Figure 5. Illustration of sperm migration through narrow inter-luminal gaps in UTJ and various size of accumulated sperm in the female reproductive tract. (**A** and **B**) The pointed sperm hook and thin head shape may assist sperm in passing through narrow gaps between mucosal folds during their migration through the UTJ (Movie S9A). Scale bar: 50 µm. (**C**) Sperm can only migrate through the UTJ when the luminal space is extended due to oviductal contraction and relaxation in the UTJ. (**D**) Various sizes of sperm accumulations (sperm trains) in the uterus. Sperm trains (or sperm assemblage) were not observed to swim faster than individual sperm in the uterus. Scale bar: 100 µm. (**E**) Accumulations of sperm in the oviduct, including the UTJ and isthmus, were primarily composed of dead and inactive sperm. These accumulated sperm may obstruct the migration of other active sperm or could cause damage to live sperm. Scale bar: 50 µm. Note that due to a lack of fluorescence, the principal and terminal pieces of sperm in all illustrated diagrams do not represent the actual shape and beating motion of the sperm tail.

Discussion

Our real-time deep tissue imaging enabled by two-photon microscopy suggests that the mouse sperm hook may (i) facilitate sperm interaction with the epithelium for better navigation and (ii) provide an anchor-like role that assists temporary fixation of sperm onto the epithelium. Based on the observations, we propose that the function of sperm hook in house mice is to facilitate sperm migration by interacting with the female reproductive tract [5,10,27], rather than facilitating sperm train formation [2,3]. We observed that sperm swim along the reproductive

tract epithelia while their apical hook interacts with the epithelia (surface). The sperm head was also observed to play an important role by providing an anchor-like role in resisting endogenous fluid flow in the female reproductive tract. We did not observe that the formation of sperm trains resulted in faster and straighter swimming. Instead, we noted instances where the accumulation of dead or damaged sperm occurred, which is potentially influenced by the apical hook and shape of the sperm head. Such aggregates of dead or damaged sperm can subsequently obstruct the migration of other sperm from the same male or other males.

The evolution of sperm characteristics and the function of the sperm hook in the house mouse is a complex process that may have been influenced by several factors. Although we cannot draw definitive conclusions from this study alone, it appears that sperm competition between ejaculates may have been a significant driving forces influencing sperm head morphology and behaviour [28]. However, cryptic female choice [29,30] is also likely to have played a crucial role in shaping the evolution of sperm head shape and sperm kinetic characteristics in mice.

As demonstrated in this study, the CT that controls sperm entry into the UTJ is an important barrier for sperm selection. If sperm passage through the CT is too easy, associated risks such as polyspermy or pathogen transmission that incur fitness costs for females may increase [31,32]. Therefore, the number of sperm passing through the CT may be balanced by the conflict between the two sexes in each rodent species depending on their mating systems. This conflict could result in an evolutionary arms race between sperm fertilization ability, including swimming speed, and the sperm selection process, including physio-chemical barriers, by the female reproductive tract [33–35].

In this study, we did not find evidence of sperm cooperation via sperm trains that aid faster sperm swimming. However, we discovered a new form of potential sperm cooperation – synchronised sperm beating that may be facilitated by unidirectional sperm clustering – in live ex-vivo samples. Unidirectional sperm clustering and its possible role in sperm migration were also suggested in a previous study with fixed and tissue-cleared samples and in-vitro sperm analysis [12]. Together with the findings in the previous study, this new form of sperm cooperation provides insight into how asymmetrical sperm heads might have evolved in rodent species and offers an opportunity to integrate the two hypotheses about the function of the sperm hook – hook for sperm cooperation to outcompete other sperm [2,3,36] and for better migration by facilitating sperm-epithelia interaction [4,5].

For example, we observed that the apical sperm hook enabled hooking and clustering of sperm at the CT (and crypts) in the uterus. This observation suggests a role for the sperm hook in facilitating interactions between sperm and epithelia in the female reproductive tract. After successful anchoring and spontaneous unidirectional re-arrangement of sperm at the CT, these sperm could exhibit synchronised beating. We also showed that such synchronised sperm beating generated enough directional flow to push off other sperm and prevent other sperm from reaching and attaching to epithelia at the CT. Therefore, unidirectional clustering of sperm can function as a preventive barrier actively blocking entry of rival sperm from the same male or even from other males into the oviduct. These results suggest that synchronised beating resulting

from unidirectional clustering can be a form of cooperation by sperm from a single male [12], helping us to integrate the two hypotheses.

Further investigation on sperm behaviour inside the female reproductive tract using real-time deep tissue imaging as in the current study will provide more important data on interactions between sperm and the female reproductive tract. This could potentially help us better understand not only sperm competition and cryptic female choice in mouse reproduction but also in other species including humans. While current assessments of sperm health generally involve measuring their count, movement, and shape after extraction, our study suggests that analysing active interactions between sperm and the female reproductive tract is important and warrants further exploration. Given the significance of sperm health for fertility, this work not only highlights the importance of interactions between sperm and female reproductive tract in successful migration but also opens new avenues for understanding different causes of infertility and possible targets for treatment.

Materials and Methods

Custom-built two-photon microscope

To observe sperm behaviour in the female mouse reproductive organ, we built a video rate (30 frames/second at 512 x 512 pixel resolution) Two-Photon Laser Scanning Fluorescence Microscope (2PLSM; Fig. S1). A tunable femtosecond pulse laser (Chameleon, Discovery) was tuned to a choice of wavelengths from 960, 970, 980 and 1000 nm to simultaneously excite GFP and Ds-Red for sperm imaging and for autofluorescence imaging of the reproductive tract. Imaging quality was found to be similar for these wavelength ranges. All images were taken using a water dipping low magnification high NA objective lens (Nikon 16X, 0.8NA). Video-rate imaging was achieved using a resonant Galvo scanning mirror system oscillating at 8 kHz. The laser power was actively controlled using a Pockels cell. Synchronization between the Galvos, sample/objective stages, Pockels cell, photomultiplier tubes (PMTs), and the data acquisition systems were controlled using ScanImage, ver. SI2021.1.0 [37].

Mice preparation and mating

We used two male transgenic mice lines for mating experiments. We purchased B6D2-Tg(CAG/Su9-DsRed2, Acr3-EGFP)RBGS002Osb male mice that express DsRed in the mitochondria at sperm midpiece and EGFP in the sperm acrosome from Riken BRC, Japan, depositor: M. Ikawa [13]. We then conducted in vitro fertilization to produce specific pathogen-free (SPF) F1 mice. The fertilized eggs (2-cell stage embryos) were then artificially inseminated into SPF wild-type C57BL/6J females. After we confirmed successful production of transgenic F1 male mice by PCR, we confirmed the SPF status and formed two breeding colonies with the transgenic F1 males under the SPF condition. One breeding colony comprised two wild-type C57BL/6J females to better reproduce F2 generation. We also made breeding colonies that consisted of a transgenic C57BL/6J female, Cx3cr1tm2.1(cre/ERT2)Litt/WganJ (JAX stock #021160, Cx3cr1 female) that expresses EYFP in microglia [38] to test whether sperm functionality changes in other mice including double-transgenic mice. When F2 mice got older than 6 weeks, they were transferred to another room where mating experiments were conducted.

After transfer, each male mouse for mating experiments was single-caged. We used the F2 males that derived from both colonies that had the two genes (CAG/Su9-DsRed2 and Acr3-EGFP; RBGS male) or three genes (CAG/Su9-DsRed2, Acr3-EGFP, and Cx3cr1; RBGS-Cx3cr1 male) for mating experiments. We could not find any phenotypic difference in the sperm of the two strains – sperm from both strains expressed red fluorescence at the midpiece and green fluorescence at the acrosome at the head. We confirmed that both strains of F2 males were fertile, and their sperm also successfully migrated through the female reproductive tract, from the uterus to the ampulla.

In total, we used 3 males that successfully mated with females due to space limits in the experimental room (Table S1). The 3 males were used repeatedly for all mating experiments in the current study except one vasectomized RBGS-Cx3cr1 male that was used only once for comparison of the CT structure for virgin and non-virgin female mice (Table S2). All mice were kept under a housing condition that allows free access to food and water with 12 hours of light and dark cycle (lighting from 6 to 18 o'clock, dark from 18 to 6 o'clock). Mating experiments were done under light conditions from 9 am to 12 pm for three hours. Oestrus was induced by exposing male bedding materials (wood shavings) that consisted of male excretion to females older than 8 weeks. Three to seven days after exposure to the bedding materials, oestrus was checked daily following previously established protocols [39]. When we found oestrous females, we relocated one or two females to a single-caged male. When males showed no interest in the female (no mounting attempts) or the female rejected the male's mounting attempt for the first 10 minutes, we returned the female to its original cage. The returned females were not exposed to other males until the next mating trial on the next day or one week later. All females in the experiments had no birth records before successful copulatory plug-confirmed mating. However, some of them probably had multiple oestrous cycles given our multiple oestrus-inducing trials. We did not limit the age of females and males for our experiments to minimize the number of sacrificed animals. We observed the male's mating until we could observe ejaculation. To confirm male ejaculation, we checked the copulatory plug from the female genitalia after we observed ejaculatory behaviour – the male stops thrusting and holds the female for about 5 to 10 seconds when it ejaculates. After this ejaculatory behaviour, we waited for 2 minutes and if the male did not exhibit further mounting, we checked the copulatory plug from the female genitalia. When the male ejaculated, we kept them together for up to 3 hours then took out the female for imaging experiments.

Ex vivo imaging with two-photon microscopy

Female mice were sacrificed by cervical dislocation after anaesthesia using 2% isoflurane inhalation which usually took less than 5 minutes. After euthanasia, the female reproductive tract with the copulatory plug was excised and washed with Dulbecco's modified Eagle's medium [40] (DMEM; GibcoTM, cat. No. 21063029). After washing, the reproductive tract was attached to a tissue culture dish with tissue adhesive (3M Vetbond 1469SB). After attachment, we filled the dish with 37°C preheated medium that contained an equal amount of DMEM and modified human tubal fluid (mHTF; Fujifilm Irvine Scientific, cat. ID. 90126) medium. All media were stored for at least 1 hour in a 37°C preheated incubator with 5% of CO_2 concentration before use. The culture dish was then placed on the 37°C preheated metal mount of the two-photon

microscope and imaged with varying laser power for different depths. Most of the images were taken with 512 x 512 pixel image size at 30 fps (262,144 pixels per frame). Multicolour imaging was performed where each frame of the image has two colour channels (red and green). If needed, we could increase the frame rate up to 110 fps or higher by reducing the acquired image size to 128 x 128 (16,384 pixels per frame). We conducted observation for about 3 to 6 hours. During our observation, the uterus continued contraction and relaxation cycles.

To image the entire depth of the reproductive tract, we applied tissue clearing to investigate the structure of the UTJ entrance (or colliculus tubarius, CT) using the C-Match solution (RI = 1.46, Crayon technologies, Korea). In brief, the tissue was first washed 3 times in PBS and fixed in 4% paraformaldehyde for 3 hours at 4°C in a refrigerator. After fixation, we washed the tissue 3 times with PBS and the absorbed residual PBS using paper towels. We then added C-Match to the sample and waited overnight and imaged it on the next day with the sample submerged in C-Match. We imaged three cleared samples from three different females. In one sample (Fig. 3A), only the intramural UTJ part was excised from one unmated transgenic C57BL/6J female mouse – a hybrid female that was delivered from Cx3cr1 female and Thy1 male (JAX stock #030526) called Tg(Thy1-jRGECO1a)GP8.31Dkim [41]. Another sample was from a female that was mated with a vasectomized RBGS-Cx3cr1 male. In this sample, the whole female reproductive tract was excised with the copulatory plug, so the intramural UTJ was covered by the uterus. This sample was used to compare the UTJ for virgin and non-virgin females. The final sample was from a wild-type female that was mated with an RBGS-Cx3cr1 male. For cleared tissue imaging, we acquired 3D volume images with 2 um Z-axis step size while averaging 20 (first sample) or 30 images (second sample) per slice to increase the signal to noise ratio using autofluorescence of the reproductive tract tissue.

Sperm tracking and speed measurement

We used Fiji [15] to process acquired images and its plugin, called TrackMate [17,18] to track sperm trajectory in the uterus. We extracted trajectories from 60 sequential images (duration 2 seconds) for sperm tracking when uterus movement was the smallest. We also used Turboreg [42], an ImageJ plugin, to realign the images when there was a shift between images due to uterine movement. Additionally, out of eight stacked images, we cropped three to obtain a straight view of the uterine wall. After preparing the images, we targeted the sperm head to track sperm as the sperm head expressed EGFP which was easy to track. We used Thresholding Detector to select sperm heads and LAP Tracker to trace sperm trajectories using the TrackMate plugin. We also adjusted parameter values in the plugin to better select sperm trajectories. Our final parameter values are as follows: head radius (> 0.75 µm), frame-to-frame linking (10 ~ 11 µm), track segment gap closing (max distance: 10 ~ 11 µm, max frame gap: 2), number of spots in track (> 6), and max distance travel (2.5 µm). When there were artificial trajectories that were not from sperm, we manually removed the track. If the original parameters could not detect well or had too many false tracks, we adjusted two parameters; frame-to-frame linking (up to 12 µm), and track segment gap closing (only max distance up to 12 µm). We also tracked the trajectories of sperm trains using the same parameters and settings. However, to reduce computation time and prevent mis-tracking of non-sperm cells, we cropped the images and utilized 100x100 pixel

images that contain the entire trajectory of each sperm train as well as other unlinked single spermatozoa.

To calculate sperm speed in relation to the distance from the uterine wall, we need to define the uterine wall. To define the uterine wall, we first selected images with straighter uterine wall and projected the extracted 60 sequential images into one plane by taking the maximum intensity projection with some adjustment of brightness and contrast using Fiji. For some images taken at a low magnification level that contained curved uterine walls, we used parts of the field of view that contained straight walls appropriate for our analysis. Next, we used the object selection tool of Adobe Photoshop CC (23.1.0 version) to automatically select the walls from the projected images. We then extracted the uterine wall image layer and pasted it to a blank image with white background. Finally, we extracted the wall coordinates by selecting the non-zero-valued pixels that formed the boundary of the uterine wall (blue coloured area in Fig. S2A). The boundary coordinates were converted to a micrometre scale based on the magnification and image resolution to normalize the units between different images obtained with different magnification factors. We fitted the uterine wall coordinates using linear regression. The fitted linear regression line was considered the uterine wall of each female (① in Fig. S2B) and used to calculate the distance and angle (radian) between sperm and the wall.

We measured the distance between sperm and the uterine wall by calculating the minimum distance between the mid-point of each sperm trajectory and the fitted line of the uterine wall (② in Fig. S2B). The angle between a sperm trajectory and the uterine wall was calculated by measuring the angle between the fitted line and a straight line that passed the first and last spots of the trajectory (③ in Fig. S2B). We then computed sperm progression speed parameters used in CASA [19] using our sperm tracking data using the TrackMate plug-in. We first calculated curvilinear velocity, VCL by dividing the total distance travelled (µm) by total track time – the time (second) taken from the first point (spot) to the last point in a sperm trajectory. The straight line velocity, VSL was calculated by dividing the track displacement – the distance between the first and last spots of a sperm trajectory – by the total track time (second). We also calculated the linearity of forward progression, LIN of sperm by dividing VSL by VCL (range 0 to 1). Along with the above CASA-used parameters, we defined a new parameter, the straight line-to-sideward movement ratio (SWR) to estimate sperm migration linearity by comparing forward and sideward moving distances. SWR was calculated by dividing the track displacement (µm) of a sperm trajectory by the maximum sideward movement distance (µm) – the maximum distance between two parallel lines passing each point (spot) that parallel to the track displacement line (④ in Fig. S2B). Further information on the terms and parameters of the TrackMate plug-in used in the current paper is also described in a paper and manual by the developers [17,18].

Statistical analysis

All statistical analyses were done using R, version 4.3.0 [16]. To estimate sperm swimming speed and linearity in relation to the uterine wall, we used data from 8 copulation experiments between 8 females and 3 males. We ran 4 generalized linear mixed models to test whether sperm move faster and straighter when they migrate along the uterine wall. We used log-transformed VCL, VSL, LIN, and SWR as response variables in each model. In all models, we included the

angle and distance between the wall and sperm trajectories as explanatory variables. We also included whether we cropped the image or not (O or X) to check the effect of image cropping on the analysis. Male IDs and the date of experiments were included as random effects in all models to control possible individual variations in sperm and reproductive tract properties. All models did not violate assumptions. All full models were also compared with null models that only included random effect and all full models were significantly better than the null models. All variance influencing factors (VIFs) were less than 1.1 which indicates no serious drawback from collinearity.

References

1. Roldan ERS, Gomendio M, Vitullo AD. The evolution of eutherian spermatozoa and underlying selective forces: female selection and sperm competition. Biol Rev. 1992;67: 551–593. doi:10.1111/j.1469-185X.1992.tb01193.x
2. Moore H, Dvoráková K, Jenkins N, Breed W. Exceptional sperm cooperation in the wood mouse. Nature. 2002;418: 174–177. doi:10.1038/nature00832
3. Fisher HS, Hoekstra HE. Competition drives cooperation among closely related sperm of deer mice. Nature. 2010;463: 801–803. doi:10.1038/nature08736
4. Smith TT, Yanagimachi R. The viability of hamster spermatozoa stored in the Isthmus of the oviduct: the importance of sperm-epithelium contact for sperm survival. Biol Reprod. 1990;42: 450–457. doi:10.1095/biolreprod42.3.450
5. Firman RC, Simmons LW. Sperm competition and the evolution of the sperm hook in house mice. J Evol Biol. 2009;22: 2505–2511. doi:10.1111/j.1420-9101.2009.01867.x
6. Hook KA, Wilke LM, Fisher HS. Apical sperm hook morphology is linked to sperm swimming performance and sperm aggregation in *Peromyscus* mice. Cells. 2021;10: 2279. doi:10.3390/cells10092279
7. Helmchen F, Denk W. Deep tissue two-photon microscopy. Nat Methods. 2005;2: 932–940. doi:10.1038/nmeth818
8. Benninger RKP, Piston DW. Two-photon excitation microscopy for the study of living cells and tissues. Curr Protoc Cell Biol. 2013;59: 4111–41124. doi:10.1002/0471143030.cb0411s59
9. Keller PJ. Imaging morphogenesis: technological advances and biological insights. Science. 2013;340: 1234168. doi:10.1126/science.1234168
10. Suarez SS. Sperm transport and motility in the mouse oviduct: observations in situ. Biol Reprod. 1987;36: 203–210. doi:10.1095/biolreprod36.1.203
11. Ishikawa Y, Usui T, Yamashita M, Kanemori Y, Baba T. Surfing and swimming of ejaculated sperm in the mouse oviduct. Biol Reprod. 2016;94. doi:10.1095/biolreprod.115.135418
12. Qu Y, Chen Q, Guo S, Ma C, Lu Y, Shi J, et al. Cooperation-based sperm clusters mediate sperm oviduct entry and fertilization. Protein Cell. 2021;12: 810–817. doi:10.1007/s13238-021-00825-y

13. Hasuwa H, Muro Y, Ikawa M, Kato N, Tsujimoto Y, Okabe M. Transgenic mouse sperm that have green acrosome and red mitochondria allow visualization of sperm and their acrosome reaction *in vivo*. Exp Anim. 2010;59: 105–107. doi:10.1538/expanim.59.105
14. Díaz-García C, Akhi SN, Martínez-Varea A, Brännström M. The effect of warm ischemia at uterus transplantation in a rat model. Acta Obstet Gynecol Scand. 2013;92: 152–159. doi:10.1111/aogs.12027
15. Schindelin J, Arganda-Carreras I, Frise E, Kaynig V, Longair M, Pietzsch T, et al. Fiji: an open-source platform for biological-image analysis. Nat Methods. 2012;9: 676–682. doi:10.1038/nmeth.2019
16. R Core Team. R: A language and environment for statistical computing. Vienna, Austria: R Foundation for Statistical Computing; 2023.
17. Tinevez J-Y, Perry N, Schindelin J, Hoopes GM, Reynolds GD, Laplantine E, et al. TrackMate: an open and extensible platform for single-particle tracking. Methods. 2017;115: 80–90. doi:10.1016/j.ymeth.2016.09.016
18. Ershov D, Phan M-S, Pylvänäinen JW, Rigaud SU, Le Blanc L, Charles-Orszag A, et al. TrackMate 7: integrating state-of-the-art segmentation algorithms into tracking pipelines. Nat Methods. 2022;19: 829–832. doi:10.1038/s41592-022-01507-1
19. Amann RP, Waberski D. Computer-assisted sperm analysis (CASA): capabilities and potential developments. Theriogenology. 2014;81: 5–17. doi:10.1016/j.theriogenology.2013.09.004
20. Zaferani M, Palermo GD, Abbaspourrad A. Strictures of a microchannel impose fierce competition to select for highly motile sperm. Sci Adv. 2019;5: eaav2111. doi:10.1126/sciadv.aav2111
21. Nakanishi T, Isotani A, Yamaguchi R, Ikawa M, Baba T, Suarez SS, et al. Selective passage through the uterotubal junction of sperm from a mixed population produced by chimeras of calmegin-knockout and wild-type male mice. Biol Reprod. 2004;71: 959–965. doi:10.1095/biolreprod.104.028647
22. Suarez SS, Pacey AA. Sperm transport in the female reproductive tract. Hum Reprod Update. 2006;12: 23–37. doi:10.1093/humupd/dmi047
23. Carretero A, Ruberte J, Navarro M. Female genital organs. In: Ruberte J, Carretero A, Navarro M, editors. Morphological Mouse Phenotyping. Academic Press; 2017. pp. 227–251. doi:10.1016/B978-0-12-812972-2.50009-X
24. Yu S-X, Wu Y, Luo H, Liu Y, Chen Y-C, Wang Y-J, et al. Escaping behavior of sperms on the biomimetic oviductal surface. Anal Chem. 2023;95: 2366–2374. doi:10.1021/acs.analchem.2c04338
25. Baker RR, Bellis MA. Human sperm competition: ejaculate manipulation by females and a function for the female orgasm. Anim Behav. 1993;46: 887–909. doi:10.1006/anbe.1993.1272
26. Hino T, Yanagimachi R. Active peristaltic movements and fluid production of the mouse oviduct: their roles in fluid and sperm transport and fertilization. Biol Reprod. 2019;101: 40–49. doi:10.1093/biolre/ioz061

27. Tourmente M, Zarka-Trigo D, Roldan ERS. Is the hook of muroid rodent's sperm related to sperm train formation? J Evol Biol. 2016;29: 1168–1177. doi:https://doi.org/10.1111/jeb.12857
28. Fisher HS, Giomi L, Hoekstra HE, Mahadevan L. The dynamics of sperm cooperation in a competitive environment. Proc R Soc B Biol Sci. 2014;281: 20140296. doi:10.1098/rspb.2014.0296
29. Birkhead TR. Cryptic female choice: criteria for establishing female sperm choice. Evolution. 1998;52: 1212–1218. doi:10.1111/j.1558-5646.1998.tb01848.x
30. Eberhard WG, Lehmann GUC. Demonstrating sexual selection by cryptic female choice on male genitalia: what is enough? Evolution. 2019;73: 2415–2435. doi:10.1111/evo.13863
31. Firman RC, Simmons LW. Sperm competition risk generates phenotypic plasticity in ovum fertilizability. Proc R Soc B Biol Sci. 2013;280: 20132097. doi:10.1098/rspb.2013.2097
32. Mahabir E, Bauer B, Schmidt J. Rodent and germplasm trafficking: risks of microbial contamination in a high-tech biomedical world. ILAR J. 2008;49: 347–355. doi:10.1093/ilar.49.3.347
33. Lüpold S, Pitnick S. Sperm form and function: what do we know about the role of sexual selection? Reproduction. 2018;155: R229–R243. doi:10.1530/REP-17-0536
34. Simmons LW, Wedell N. Fifty years of sperm competition: the structure of a scientific revolution. Philos Trans R Soc B Biol Sci. 2020;375: 20200060. doi:10.1098/rstb.2020.0060
35. Firman RC, Gasparini C, Manier MK, Pizzari T. Postmating female control: 20 years of cryptic female choice. Trends Ecol Evol. 2017;32: 368–382. doi:10.1016/j.tree.2017.02.010
36. Immler S, Moore HDM, Breed WG, Birkhead TR. By hook or by crook? Morphometry, competition and cooperation in rodent sperm. PLOS ONE. 2007;2: e170. doi:10.1371/journal.pone.0000170
37. Pologruto TA, Sabatini BL, Svoboda K. ScanImage: flexible software for operating laser scanning microscopes. Biomed Eng OnLine. 2003;2: 13. doi:10.1186/1475-925X-2-13
38. Parkhurst CN, Yang G, Ninan I, Savas JN, Yates JR, Lafaille JJ, et al. Microglia promote learning-dependent synapse formation through brain-derived neurotrophic factor. Cell. 2013;155: 1596–1609. doi:10.1016/j.cell.2013.11.030
39. Byers SL, Wiles MV, Dunn SL, Taft RA. Mouse estrous cycle identification tool and images. PLOS ONE. 2012;7: e35538. doi:10.1371/journal.pone.0035538
40. Tayama K, Fujita H, Takahashi H, Nagasawa A, Yano N, Yuzawa K, et al. Measuring mouse sperm parameters using a particle counter and sperm quality analyzer: a simple and inexpensive method. Reprod Toxicol. 2006;22: 92–101. doi:10.1016/j.reprotox.2005.11.009
41. Dana H, Novak O, Guardado-Montesino M, Fransen JW, Hu A, Borghuis BG, et al. Thy1 transgenic mice expressing the red fluorescent calcium indicator jRGECO1a for neuronal population imaging in vivo. PLOS ONE. 2018;13: e0205444. doi:10.1371/journal.pone.0205444

42. Thevenaz P, Ruttimann UE, Unser M. A pyramid approach to subpixel registration based on intensity. IEEE Trans Image Process. 1998;7: 27–41. doi:10.1109/83.650848

Acknowledgments

We appreciate members of the Bio-Optics Lab and In-vivo Research Center at the Ulsan National Institute of Science and Technology for their help in building and maintaining microscopy instruments and mouse strains; particularly I. Kim, S. Park, Y. Lee, Y. Kwon, Y. Choi, H. Kim, E. Cho, and T. Asadishad. We also thank M. Okabe, G. Kang, and Y. Kawaguchi for their comments about the methods and manuscript. **Funding sources**: National Research Foundation of Korea grant 2020R1A6A3A01098226 (HR), National Research Foundation of Korea grant 2019M3E5D2A01063812 (JP), National Research Foundation of Korea grant 2021R1A2C3012903 (JP), National Research Foundation of Korea grant 2021R1A4A1031644 (JP), National Research Foundation of Korea grant RS-2023-00264980 (JP), Ministry of Science and ICT (IITP-2023-RS-2023-00259676) (JP), National Research Foundation of Korea grant 2021M3A9G8022960 (JK1, Jae-Ick Kim), National Research Foundation of Korea grant 2022M325E8017907 (JK1)

Author Contributions

Conceptualization: HR, JP, Methodology: HR, KN, YJ, SL, JK2 (Jungmo Kim), JP, Investigation: HR, KN, BL, YJ, JP, Visualization: HR, KN, YJ, JP, Funding acquisition: HR, JK1, JP, Project administration: JK1, JP, Supervision: JK1, JP, Writing – original draft: HR, JP, Writing – review & editing: all authors

Declaration of interests

Authors declare that they have no competing interests.

Data and materials availability

Raw data on sperm trajectories in the female reproductive track is available at https://figshare.com/s/82d3f991ba884af73898. Custom codes for sperm tracking data analysis written with Matlab (version R2019b) are available at https://github.com/YundonJeong/Sperm_tracking.

Supplementary Information for

The sperm hook in house mice: a functional adaptation for migration and self-organised behaviour

Heungjin Ryu[1,2]*†, Kibum Nam[1]†, Byeong Eun Lee[3]†, Yundon Jeong[1]†, Seunghun Lee[1], Jeongmo Kim[1], Young-Min Hyun[4], Jae-Ick Kim[3]*, Jung-Hoon Park[1]*

*Corresponding authors. Heungjin Ryu, Jae-Ick Kim, Jung-Hoon Park

Email: ryu.heungjin.26v@kyoto-u.jp; jikim220@unist.ac.kr; jh.park@unist.ac.kr

This file includes:

Figures S1 to S3

Tables S1 to S3

Legends for Movies S1 to S10

Other supporting materials for this manuscript include the following:

Movies S1 to S10

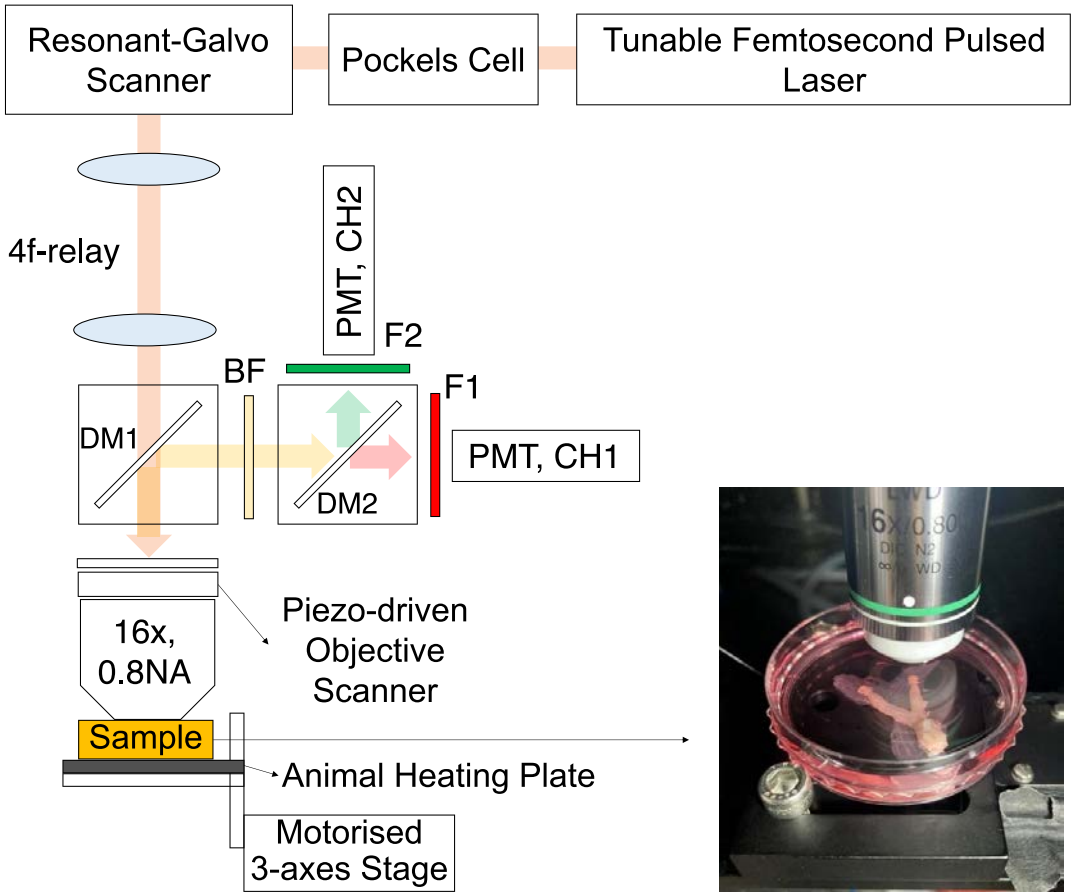

Fig. S1. Schematic diagram of the custom-built 2PSLM.

DsRed and eGFP were excited nonlinearly using a tunable high peak power femtosecond laser (Chameleon discovery/Coherent) and a water-immersion objective lens (CFI75 LWD 16X W/Nikon). The fluorescence emitted was collected by the same objective lens and detected by a pair of GaAsP photomultiplier tubes (PMT, H10770PA-40/Hamamatsu). Dichroic mirrors and filters; DM1(T735lpxrxt-UF3/Chroma), DM2(T565lxr/Chroma), BF(ET720SP-2P8/Chroma), F1(ET605/70m/Chroma), and F2(ET525/70m/Chroma) were used to split the excitation beam and emission light. A resonant-galvo scanner (RESCAN-GEN/Sutter instrument) enabled real-time fluorescence imaging of sperm behaviour at a speed of 30 frames per second for 512 pixels per line acquisition. A Pockels cell (M350-80-LA-02 KDP/Conoptics) allowed for rapid control of the laser beam intensity, homogenising the illumination across the field of view, and applying varying laser power per tissue depth. The sample position in all three dimensions was controlled by a Piezo-driven objective scanner (P-725.4CA/PI) and a motorised 3-axes stage (3DMS/Sutter instrument). A small animal heating plate (HP-4M/Physitemp) maintained the warmth of the mouse female reproductive tract at body temperatures.

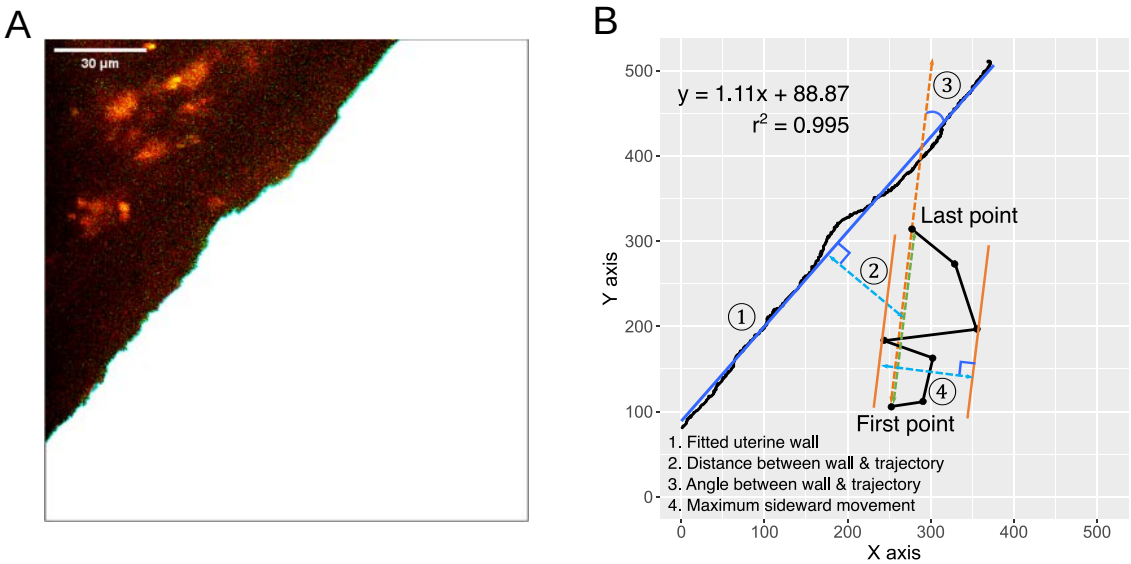

Fig. S2. Uterus wall and parameters that were used to measure sperm migration speed and linearity.

(**A**) Areas along the uterine wall that were relatively straight were selected. The boundary of these areas was identified using the object selection tool in Adobe Photoshop CC (23.1.0 version). (**B**) The uterine wall was approximated as a linear line using linear regression (①). The distance between a spermatozoon and the uterine wall was defined as the minimum distance between the midpoint of the track displacement and a sperm trajectory (②). The angle between sperm trajectories and the uterine wall was calculated as the angle (in radians) between the uterine wall (approximated line) and the straight line that connected the first and last points of a sperm trajectory – track displacement line (③). The maximum sideward movement was determined as the greatest distance between the parallel lines that aligned with the track displacement line at the positions of the sperm trajectory (④). SWR was then computed by dividing the track displacement by the maximum sideward movement.

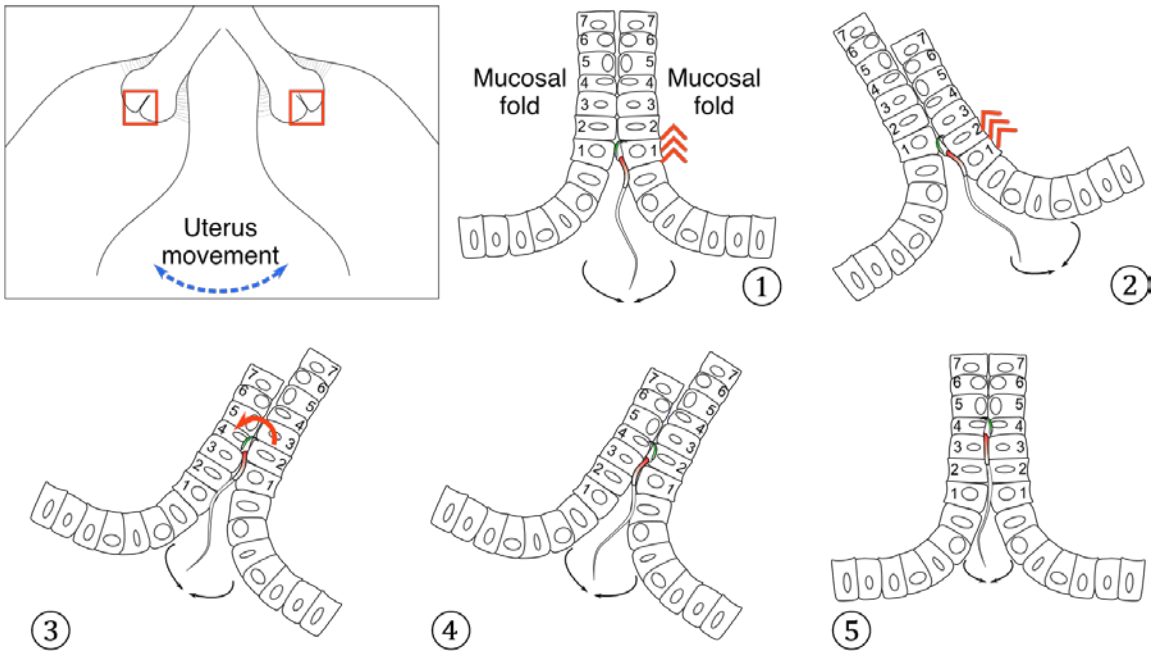

Fig. S3. A hypothetical model for sperm migration from the uterus to UTJ.
The upper left inset represents a uterine horn that moves to the left or right due to muscle contraction (exaggerated for visualization). The 5 subfigures with numbering represent zoom-in of the two red square frames in the inset. When the uterine horn moves from the centre to the right (① to ②), two facing surfaces between the two mucosal folds slide against each other. This sliding results in opening space where sperm can ascend – note that the sperm moves from cell 1 to cell 2 of the right mucosal fold (②). When the uterine horn moves from right to left (③), the two surfaces between the mucosal folds slide in opposite directions where the sperm can now reach cell 4 of the left mucosal fold. If sperm can turn over, its head can be attached to cell 4 of the left mucosal fold (④ to ⑤). Repetition of these procedures will make the sperm finally pass the CT and migration through narrow gaps between mucosal folds in intramural UTJ. This process appears to be as if sperm may slide through the space between mucosal folds when the space is too small for normal beating (Movie S5C).

Table S1. Basic information of 4 males that were used for the mating experiment.

Male ID	Date of Birth (DOB)	Genotype	Note
A (No. 838)	2021.04.21	RBGS-CX3CR1	
B (No. 3399)	2021.08.17	RBGS	
C (No. 3613)	2021.09.01	RBGS	
D (No. 3610)	2021.09.01	RBGS-CX3CR1	Vasectomized male

RBGS: CAG/Su9-DsRed2 and Acr3-EGFP, RBGS-CX3CR1: CAG/Su9-DsRed2, Acr3-EGFP, and Cx3cr1

Table S2. Mating records and the information of the females for sperm tracking.

Date of mating	DOB (female)	Age (female)	Male ID
2021-12-15	2021-09-01	15.0 weeks	A
2021-12-23	2021-07-02	24.9 weeks	B
2022-03-11	2021-05-10	43.6 weeks	A
2022-04-07	2021-08-17	33.3 weeks	A
2022-06-08	2021-10-17	33.4 weeks	C
2022-07-07	2022-02-14	20.4 weeks	C
2022-07-14	2021-10-17	38.6 weeks	A
2022-08-04	2022-02-14	24.4 weeks	A

Male ID: males (Supplementary Table 1) who mated with the subject females on the date.

Table S3. Summary results of the generalized linear mixed models (GLMM).

Each model represents sperm trajectory parameters that were log-transformed. In all models, we examined the effect of sperm to uterine wall distance (Distance from wall), angle between a sperm trajectory and uterine wall (respective angle with wall) and cropping of the acquired image (O: cropped vs X: uncropped). The GLMM for SWR showed a boundary (singular) fit warning message. However, two models that omitted one of random variables (Male or Date) did not result in any significant changes in the predictor variables ($p > 0.05$).

Model	Predictors	Estimates	SE	*t*	*P*	95% CI
VCL	(Intercept)	4.0645	0.4189	9.7028	0.001**	3.198, 4.921
	Distance from wall	-0.0094	0.0007	-12.8449	<0.001***	-0.011, -0.008
	Angle with wall	-0.0019	0.0007	-2.6255	0.009**	-0.003, 0
	Cropped (O: X)	-0.2576	0.4368	-0.5897	0.584	-1.155, 0.652
VSL	(Intercept)	3.2745	0.4277	7.6558	0.002**	2.434, 4.113
	Distance from wall	-0.0104	0.0014	-7.4718	<0.001***	-0.013, -0.008
	Angle with wall	-0.0081	0.0014	-5.9303	<0.001***	-0.011, -0.006
	Cropped (O: X)	-0.0822	0.4202	-0.1957	0.853	-0.902, 0.716
LIN	(Intercept)	-0.8236	0.1194	-6.8999	0.001**	-1.058, -0.581
	Distance from wall	-0.0009	0.0011	-0.8632	0.388	-0.003, 0.001
	Angle with wall	-0.0061	0.0010	-5.8469	<0.001***	-0.008, -0.004
	Cropped (O: X)	0.1701	0.1365	1.2459	0.273	-0.113, 0.444
SWR	(Intercept)	1.1507	0.1458	7.8917	<0.001***	0.732, 1.430
	Distance from wall	-0.0003	0.0013	-0.2149	0.830	-0.003, 0.002
	Angle with wall	-0.0108	0.0013	-8.2828	<0.001***	-0.013, -0.008
	Cropped (O: X)	0.1566	0.1720	0.9107	0.399	-0.384, 0.835

VCL: curvilinear velocity, VSL: straight-line velocity, LIN: linearity of forward progression, SWR: straight line-to-sideward movement ratio, ***: $p < 0.001$, **: $p < 0.01$, *: $p < 0.05$.

Captions for Movie S1 to S10

Movie S1.

Sperm migration in the uterus. (**A**) Most sperm within the uterine volume are moving back and forth following the flow in the uterus. (**B**) Sperm near a uterine wall (epithelium) are more active and swim faster than those in the centre of the lumen. Tracks are guides to the eye showing the instantaneous speed as different colours.

Movie S2.

The sperm hook helps sperm to determine migration directions in the uterus. (**A**) When sperm reach the uterine wall, sperm change their migration direction. Most sperm change their heading direction in a way that their apical hook faces the uterine wall (pro-wall-hook direction) which allows sperm migrate straighter along the wall. In contrast, a few sperm exhibit an opposite heading direction such that their hook faces the uterine lumen (anti-wall-hook direction). This heading direction usually results in a departure of the sperm from the wall. (**B**) Sperm are tapping along the epithelium with their hook while migrating along the uterine wall.

Movie S3.

Sperm use their hook as an anchor to be attached to the uterine epithelium. (**A**) Sperm use their hook to be attached to the uterine epithelium (sperm hooking behaviour for anchoring). The apical sperm hook also helps sperm squeeze through other sperm in confined space. (**B**) Unattached (unanchored) or loosely attached sperm may be more easily squeezed out by uterine muscle contraction or fluid flow.

Movie S4.

The entrance of intra-mural UTJ (or CT) in the uterus has small spacing (almost closed inter-fold gaps) for mouse sperm to pass through. (**A**) These closed inter-fold gaps continue for about 100 µm from the entrance of UTJ. (**B**) The existence of a copulatory plug or mating history does not influence the opening of the inter-fold gap at the UTJ entrance (UTJ entrance seen from an orthogonal perspective with respect to **A**). (**C)** Even after mating with a male with working sperm, width of inter-fold gaps does not considerably change. Only a few sperm can pass through the inter-fold gap at a time due to its narrow width. Scanning direction of the intra-mural UTJ to get images is indicated with an arrow at the right upper corner in each Movie.

Movie S5.

Sperm behaviours and the movement of mucosal folds at the entrance of UTJ (CT). (**A**) There is no upsuck-like passive sperm transfer from the uterus to UTJ. Some unanchored sperm are sometimes pulled off by muscle contraction (peristaltic movement). (**B**) Two facing mucosal folds sometimes move in an opposite direction which causes the two mucosal folds to slide against each other. Sperm may use this moment to enter UTJ from the uterus. (**C**) As the sperm head is round enough despite its apical sperm hook, sperm can move forward (head direction) by sliding through a narrow lumen between mucosal folds. However, due to the sperm hook shape (anchor), it will not be easier for sperm to move backward (tail direction).

Movie S6.

Sperm unidirectional re-arrangement in a sperm cluster at a uterine crypt. (**A**) Asymmetrical sperm head shape may facilitate sperm unidirectional re-arrangement in sperm clusters at uterine crypts and CT. The unidirectional sperm clustering then results in synchronised sperm beating that pushes out other sperm by generating fluid flow or by beating other sperm directly. (**B**) Re-arranged sperm in a cluster sometimes move together to the same direction.

Movie S7.

An enormous unidirectional sperm cluster at CT in the uterus exhibits synchronised sperm beating. The synchronised sperm beating may prevent or hinder other sperm from approaching the UTJ entrance (CT) by pushing out approaching sperm.

Movie S8.

Accumulated sperm (sperm trains) are not found to swim faster than unlinked individual sperm in the uterus. Moreover, a large sperm accumulation cannot pass the narrow luminal space near the UTJ entrance (CT). These results suggest a disadvantage of sperm trains in sperm migration from the uterus to UTJ.

Movie S9.

Various sperm behaviours in UTJ. (**A**) Sperm interact with the UTJ epithelium using their hook in various ways. They put their hook into a gap (crypt) and exhibit tapping- and stroking-like behaviour while they migrate through UTJ. (**B**) Sperm can more easily migrate when UTJ lumens get wider. Attached (anchored) sperm also beat faster when UTJ lumens get wider. (**C**) Dead or inactive sperm are accumulated in UTJ and may damage live sperm through collisions or hinder sperm migration in UTJ.

Movie S10.

The beating rate of the attached (anchored) sperm in UTJ changes over time. The speed of fluid flow and the luminal width of UTJ may be related to the beating rate.